

Imaginary part of Feynman amplitude, cutting rules and optical theorem

Yong Zhou

*Institute of High Energy Physics, Academia Sinica, P.O. Box 918(4),
Beijing 100049, China, Email: zhouy@mail.ihep.ac.cn*

We discussed the algorithm of calculating the imaginary part of Feynman amplitude and the optical theorem. We ameliorate the cutting rules in order to make it suitable for actual calculations and give accurate imaginary part of unstable particle's self-energy amplitude. The calculations of several Feynman diagrams' imaginary parts show that the ameliorated cutting rules agrees with the conventional integral algorithm very well. The investigations help us to find that the optical theorem is broken by the singularities of Feynman amplitudes. Furthermore the calculations of the decay widths of the physical processes $t \rightarrow cZ$ and $b \rightarrow s\gamma$ show that the optical theorem leads to the physical results gauge-parameter dependent.

PACS numbers: 12.38.Bx, 11.80.Cr, 11.55.-m

I. INTRODUCTION

The singularities of Feynman propagators have contribution to the imaginary part of physical amplitudes [1, 2]. One of the way to calculate this contribution is the causal perturbative theory [1]. Another way is called as cutting rules [2], proposed by Cutkosky. In this manuscript we mainly discuss the prescription of the cutting rules. Although it is a well-defined algorithm, the cutting rules doesn't give an integrative prescription to calculate this contribution, nor it reveals the physical meaning of this contribution. So we want to ameliorate the cutting rules to make it suitable for actual calculations and investigate its physical meaning.

On the other hand, the optical theorem has given a strong constraint on the imaginary part of physical amplitudes. Whether they agrees with each other hasn't been clearly investigated? Here we will discuss their relationship and investigate the origin of the optical theorem. The arrangement of this paper is: firstly we discuss how to ameliorate the cutting rules; then we calculate some Feynman diagrams' imaginary parts to see the homology of the ameliorated cutting rules and the conventional integral algorithm; in Sect.4 we investigate the breaking of the optical theorem by the singularities of physical amplitudes; in Sect.5 we calculate the norm squares of two physical amplitudes: top quark decaying into charm quark and gauge boson Z and bottom quark decaying into strange quark and photon, to investigate the gauge dependence of the physical results under the optical theorem and the ameliorated cutting rules; lastly we give our conclusion in Sect.6.

II. AMELIORATE THE CUTTING RULES

We usually encounter branch cut in Feynman parameter integrals in conventional Feynman amplitude calculations. It can be divided into two kinds: one comes from the dimensional regularization [3], i.e. comes from the term $\ln(\Delta - i\varepsilon)$ when $\Delta < 0$, the other comes from the singularities of Feynman parameter integrals, i.e. comes from the term $1/(\Delta - i\varepsilon)^N$ when $\Delta = 0$, where ε is a positive infinitesimal quantity and Δ comes from the Feynman parametrization, e.g. at one-loop level

$$\int d^4k B A_1^{-1} \cdots A_N^{-1} = (N-1)! \int \prod (d\alpha) d^4l B D^{-N} \delta(1 - \tilde{\alpha}),$$

where B is an arbitrary polynomial, $A_i = q_i^2 - M_i^2 + i\varepsilon$, $D = \sum_{i=1}^N \alpha_i A_i \equiv l^2 - \Delta + i\varepsilon$ (l is the linear combination of k and other momentums and Δ is free of loop momentum k), and $\tilde{\alpha} = \sum \alpha_i$. Both of the two branch cuts have contributions to the imaginary part of Feynman amplitude. We can calculate the contributions either by Feynman parameter integrals, or by the cutting rules. Consider the two-point Green function

$$D_F(x-y) = \int \frac{d^4p}{(2\pi)^4} \frac{i}{p^2 - m^2 + i\varepsilon} e^{-ip \cdot (x-y)}, \quad (1)$$

there are two singularities $p_0 = \pm(\sqrt{p^2 + m^2} - i\varepsilon)$ in the denominator. They represent the actions of the on-shell particle propagating from point y to x or from point x to y respectively. The cutting rules is just the algorithm of calculating the contribution of these actions to Feynman amplitudes, but it isn't suitable for actual calculations because it stipulates that only one of the two singularities in Eq.(1) has contribution to Feynman amplitude, however,

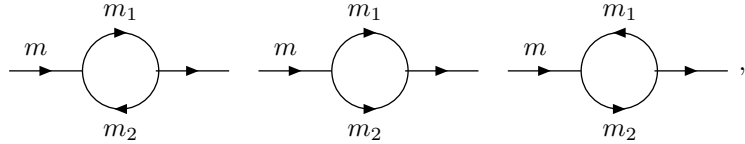
it doesn't tell which singularity is the case. So we need to ameliorate the cutting rules. We begin from the study of the one-loop self-energy amplitude. If keeping all of the singularities' contributions, we have according to the cutting rules

$$Im(-i) \int \frac{d^4 k}{(2\pi)^4} \frac{1}{k^2 - m_1^2 + i\varepsilon} \frac{1}{(k-p)^2 - m_2^2 + i\varepsilon} = \frac{\sqrt{m^4 + m_1^4 + m_2^4 - 2m^2m_1^2 - 2m^2m_2^2 - 2m_1^2m_2^2}}{16\pi m^2} \times (\theta[m_1 - m - m_2] + \theta[m - m_1 - m_2] + \theta[m_2 - m - m_1]), \quad (2)$$

where the out-line momentum p satisfies $p^2 = m^2$ and θ is the Heaviside function. According to Breit-Wigner formula the imaginary part of unstable particle's self-energy amplitude is proportional to its decay width [4]:

$$Im\mathcal{M}(p \rightarrow p) = m\Gamma. \quad (3)$$

One can easily see that only the second term of the r.h.s of Eq.(2) satisfies Eq.(3), the other terms violate it. Thus our work is to find a prescription to remove the incorrect contributions. In order to clearly discuss this question we use three diagrams to represent the three terms in Eq.(2),



where the arrow denotes the propagator with it is cut and the momentum q on it satisfies the condition $q_0 = \sqrt{\mathbf{q}^2 + M^2}$ (M is the mass of the propagator). We call such momentum propagating direction denoted by the arrow direction as *on-shell* propagating direction. Obviously the three diagrams represent the three terms in Eq.(2) in turn. Only the second diagram is accepted according to the above discussion. The important difference between the second and the other diagrams is that the arrow directions are inverse in the momentum loop in the second diagram, but are equi-directional in the momentum loops in the other diagrams. We can assume that the cuts which has contribution to Feynman amplitude must satisfy such condition: the *on-shell* propagating directions are inverse in every momentum loop. If this hypothesis is true, the momentum-energy of the cut propagators will not be provided by the virtual loop momentums, but by the incoming particles. Obviously there are at most two cut propagators occurring in each momentum loop based on this hypothesis. So each momentum loop can only be cut twice or be not cut, because we know that cutting once is equivalent to perform the conventional loop momentum integral. Besides, according to the mathematical formula (where A is a real number and P is Cauchy principle value)

$$\frac{1}{A \pm i\varepsilon} = P \frac{1}{A} \mp i\pi\delta(A), \quad (4)$$

the replacement in cutting rules should be changed to $1/(p^2 - m^2 + i\varepsilon) \rightarrow -i\pi\delta(p^2 - m^2)$. We also notice that when we integrate each cut loop momentum in the complex plane, all the singularities in it will be calculated twice since there are two-time integrations of the four components of loop momentum for the two delta functions. So the final result must be multiplied by a factor 2^n , where n is the number of the cut momentum loops. For the uncut propagators, since their singularities have no contribution to Feynman amplitude, they should be replaced by their Cauchy principle values. Summing up all the above discussions the ameliorated cutting rules should be:

1. Cut through the Feynman diagram in all possible ways such that the cut propagators can simultaneously be put on mass shell and their *on-shell* propagating directions be reverse in every cut momentum loop; keep only two cuts in each cut momentum loop.
2. For each cut propagator with definite *on-shell* propagating direction, replace $1/(p^2 - m^2 + i\varepsilon) \rightarrow -i\pi\theta[p_0] \delta(p^2 - m^2)$ (where the momentum p is along the *on-shell* propagating direction), for each uncut propagator, apply Cauchy principle value to it, then multiplied by 2^n where n is the number of the cut momentum loops, then perform the loop integrals.
3. Sum the contributions of all possible cuts.

The above discussions are very abstract. So we give some illustrations in Fig.1-5. We note that the arrows in Fig.1-5 represent the same meaning as the ones in the diagram below Eq.(3). In order to explain the ameliorated cutting rules we give two conditions in Fig.2.

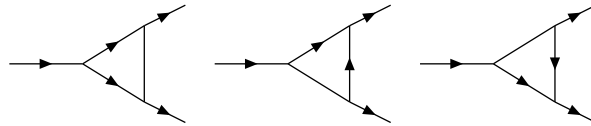


FIG. 1: Cuts of one-loop three-point irreducible Feynman diagram.

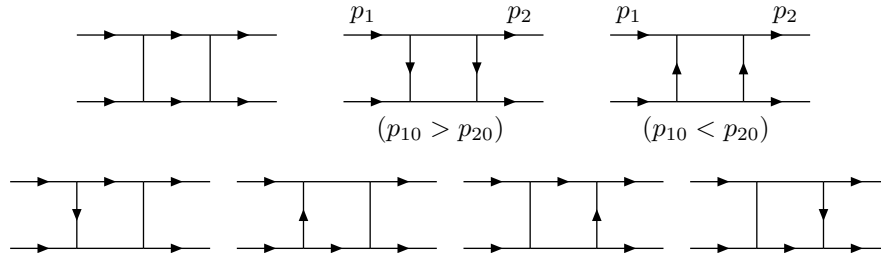


FIG. 2: Cuts of one-loop four-point irreducible Feynman diagram.

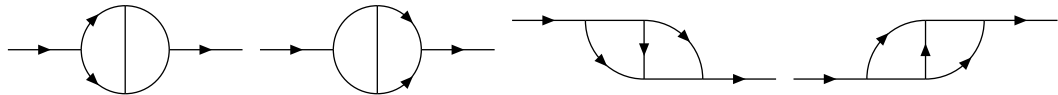


FIG. 3: Cuts of a two-loop two-point irreducible Feynman diagram.

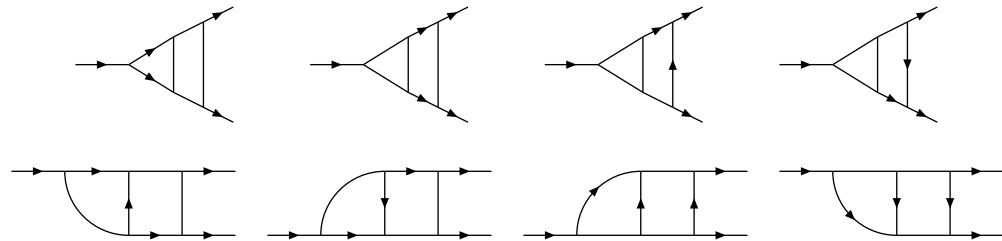


FIG. 4: Cuts of a two-loop three-point irreducible Feynman diagram.

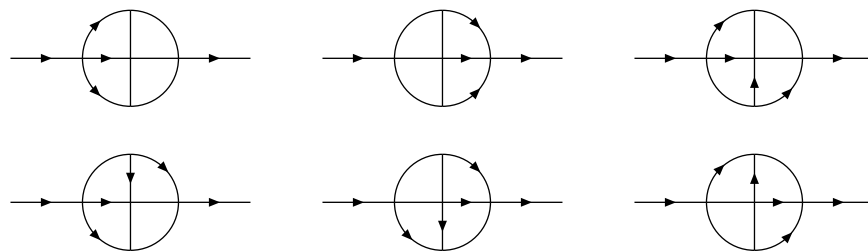


FIG. 5: Cuts of a four-loop two-point irreducible Feynman diagram.

Since each cut contributes an imaginary factor i to Feynman amplitude, all of the cut diagrams in Fig.1-5 contribute imaginary part to Feynman amplitudes. This agrees with our knowledge.

III. COMPARISON OF THE CUTTING RULES AND THE CONVENTIONAL INTEGRAL ALGORITHM

It is known that the contribution of the propagator's singularities to Feynman amplitude can be directly calculated by the conventional integral algorithm, i.e. by the Feynman parametrization, wick rotation and dimensional regularization. Here we give four examples to see whether the results obtained by the ameliorated cutting rules agrees with

the ones obtained by the conventional integral algorithm. Firstly we consider the case of the branch cut coming from the dimensional regularization. We calculate a simple two-loop two-point irreducible Feynman diagram. Under the conventional integral algorithm we have

$$\begin{aligned}
Im \xrightarrow{p, m} \text{Feynman Diagram} &= Im \int \frac{d^D k_1}{(2\pi)^D} \frac{d^D k_2}{(2\pi)^D} \frac{1}{k_1^2 - m_1^2 + i\varepsilon} \frac{1}{k_2^2 - m_1^2 + i\varepsilon} \frac{1}{(k_1 + k_2 - p)^2 - m_1^2 + i\varepsilon} \\
&= \frac{1}{256\pi^4} Im \int_0^1 dx \int_0^1 dy \ln B (A - 2m^2 y) \left(\frac{2}{\epsilon} - 2\gamma + \ln 16\pi^2 + \ln y - \ln x(1-x) - \ln B \right) \\
&= -\frac{1}{256\pi^3} \int_0^1 dx \int_0^1 dy (A - 2m^2 y) \left(\frac{2}{\epsilon} - 2\gamma + \ln 16\pi^2 + \ln y - \ln x(1-x) - 2\ln|B|\theta[-B] \right) \\
&= \frac{1}{128\pi^3} \int_{x_1}^{x_2} dx \left(\frac{A\sqrt{A^2 - 4m^2 m_1^2}}{4m^2} - m_1^2 \ln \frac{A + \sqrt{A^2 - 4m^2 m_1^2}}{2mm_1} \right) \theta[m - 3m_1], \tag{5}
\end{aligned}$$

where the outer-line momentum p satisfies $p^2 = m^2$, $\epsilon = 4 - D$, γ is the Euler constant, and

$$\begin{aligned}
A &= m^2 + m_1^2 - \frac{m_1^2}{x(1-x)}, \\
B &= m^2 y^2 - A y + m_1^2, \\
x_{1,2} &= \frac{m - m_1 \mp \sqrt{m^2 - 2mm_1 - 3m_1^2}}{2(m - m_1)}. \tag{6}
\end{aligned}$$

In Eq.(5) we have used the formula $\ln \Delta = \ln |\Delta| - i\pi\theta[-\Delta]$. On the other hand, under the ameliorated cutting rules we also have

$$\begin{aligned}
Im \xrightarrow{p, m} \text{Feynman Diagram} &= Im \int \frac{d^4 k_1}{(2\pi)^4} \frac{d^4 k_2}{(2\pi)^4} \frac{1}{k_1^2 - m_1^2 + i\varepsilon} \frac{1}{k_2^2 - m_1^2 + i\varepsilon} \frac{1}{(k_1 + k_2 - p)^2 - m_1^2 + i\varepsilon} \\
&= \frac{1}{64\pi^5} \int d^4 k_1 d^4 k_2 \theta[k_{10}] \delta(k_1^2 - m_1^2) \theta[k_{20}] \delta(k_2^2 - m_1^2) \theta[p_0 - k_{10} - k_{20}] \delta((p - k_1 - k_2)^2 - m_1^2) \\
&= \frac{1}{64m\pi^3} \int_{m_1}^{\frac{m^2 - 3m^2}{2m}} dx \sqrt{(mx + m_1^2)^2 - \frac{m_1^2(m^2 - m_1^2)^2}{m^2 + m_1^2 - 2mx}} \theta[m - 3m_1]. \tag{7}
\end{aligned}$$

Through numerical calculations we find Eq.(7) is equal to Eq.(5). The concrete results are shown in Fig.6.

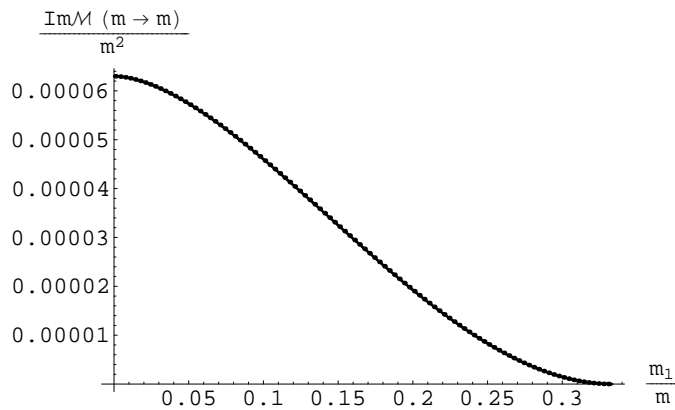


FIG. 6: Results of Eq.(5) and Eq.(7).

Secondly we consider the case of the branch cut coming from the singularities of Feynman parameter integrals. We give two examples. The first example is the calculation of a one-loop three-point irreducible Feynman diagram.

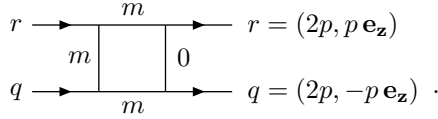
Basing on the conventional integral algorithm and Eq.(4) we have

$$\begin{aligned}
& Im(-i) \int \frac{d^4 k}{(2\pi)^4} \frac{1}{k^2 - m_1^2 + i\varepsilon} \frac{1}{(k - p_1)^2 - m_1^2 + i\varepsilon} \frac{1}{(k - p_1 - p_2)^2 - m_1^2 + i\varepsilon} \\
&= -\frac{1}{16\pi^2} Im \int_0^1 dx \int_0^{1-x} dy \frac{d y}{m_a^2 x^2 + m_b^2 y^2 + m_a^2 x y - m_a^2 x - m_b^2 y + m_1^2 - i\varepsilon} \\
&= -\frac{1}{16\pi} \int_0^1 dx \int_0^{1-x} dy \delta(m_a^2 x^2 + m_b^2 y^2 + m_a^2 x y - m_a^2 x - m_b^2 y + m_1^2) \\
&= \begin{cases} \frac{1}{16\pi m_a \sqrt{m_a^2 - 4m_b^2}} \ln \left[\frac{m_a^2 - 2m_b^2 - \sqrt{(m_a^2 - 4m_b^2)(m_a^2 - 4m_1^2)}}{m_a^2 - 2m_b^2 + \sqrt{(m_a^2 - 4m_b^2)(m_a^2 - 4m_1^2)}} \left(\frac{m_a m_b + \sqrt{(m_a^2 - 4m_b^2)(m_b^2 - 4m_1^2)}}{m_a m_b - \sqrt{(m_a^2 - 4m_b^2)(m_b^2 - 4m_1^2)}} \right)^2 \right] & \forall m_1 \in (0, \frac{m_b}{2}), \\ \frac{1}{16\pi m_a \sqrt{m_a^2 - 4m_b^2}} \ln \frac{m_a^2 - 2m_b^2 - \sqrt{(m_a^2 - 4m_b^2)(m_a^2 - 4m_1^2)}}{m_a^2 - 2m_b^2 + \sqrt{(m_a^2 - 4m_b^2)(m_a^2 - 4m_1^2)}} & \forall m_1 \in (\frac{m_b}{2}, \frac{m_a}{2}), \\ 0 & \forall m_1 \in (\frac{m_a}{2}, \infty), \end{cases} \quad (8)
\end{aligned}$$

where the outer-line momentum p_1 and p_2 satisfy $p_1^2 = p_2^2 = m_b^2$, $(p_1 + p_2)^2 = m_a^2$. Basing on the ameliorated cutting rules we also have (see Fig.1)

$$\begin{aligned}
& Im(-i) \int \frac{d^4 k}{(2\pi)^4} \frac{1}{k^2 - m_1^2 + i\varepsilon} \frac{1}{(k - p_1)^2 - m_1^2 + i\varepsilon} \frac{1}{(k - p_1 - p_2)^2 - m_1^2 + i\varepsilon} \\
&= P \int \frac{d^4 k}{8\pi^2} \left[\frac{\theta[k_0] \delta(k^2 - m_1^2) \theta[p_{10} + p_{20} - k_0] \delta((p_1 + p_2 - k)^2 - m_1^2)}{(k - p_1)^2 - m_1^2} + \frac{\theta[k_0] \delta(k^2 - m_1^2) \theta[p_{10} - k_0] \delta((p_1 - k)^2 - m_1^2)}{(k - p_1 - p_2)^2 - m_1^2} \right. \\
&\quad \left. + \frac{\theta[k_0 - p_{10}] \delta((k - p_1)^2 - m_1^2) \theta[p_{10} + p_{20} - k_0] \delta((p_1 + p_2 - k)^2 - m_1^2)}{k^2 - m_1^2} \right] \\
&= \frac{\theta[m_a - 2m_1]}{16\pi m_a \sqrt{m_a^2 - 4m_b^2}} \ln \left| \frac{m_a^2 - 2m_b^2 - \sqrt{(m_a^2 - 4m_b^2)(m_a^2 - 4m_1^2)}}{m_a^2 - 2m_b^2 + \sqrt{(m_a^2 - 4m_b^2)(m_a^2 - 4m_1^2)}} \right| \\
&\quad + \frac{\theta[m_b - 2m_1]}{8\pi m_a \sqrt{m_a^2 - 4m_b^2}} \ln \left| \frac{m_a m_b + \sqrt{(m_a^2 - 4m_b^2)(m_b^2 - 4m_1^2)}}{m_a m_b - \sqrt{(m_a^2 - 4m_b^2)(m_b^2 - 4m_1^2)}} \right|. \quad (9)
\end{aligned}$$

Eq.(9) agrees with Eq.(3.24) of Ref.[5]. Obviously Eq.(9) is equal to Eq.(8). The second example is the calculation of a one-loop four-point irreducible Feynman diagram as shown below:



Under the conventional integral algorithm and Eq.(4) we have

$$\begin{aligned}
& Im(-i) \int \frac{d^4 k}{(2\pi)^4} \frac{1}{k^2 + i\varepsilon} \frac{1}{(k - q)^2 - m^2 + i\varepsilon} \frac{1}{k^2 - m^2 + i\varepsilon} \frac{1}{(k + r)^2 - m^2 + i\varepsilon} \\
&= \frac{1}{16\pi^2} Im \int_0^1 dx \int_0^{1-x} dy \int_0^{1-x-y} dz \frac{d z}{(3p^2 x^2 + 3p^2 y^2 - 10p^2 x y - 3p^2 x - 3p^2 y - m^2 z + m^2 - i\varepsilon)^2} \\
&= \frac{1}{16\pi^2 m^2} Im \int_0^1 dx \int_0^{1-x} dy \left[\frac{1}{(3p^2 x^2 + 3p^2 y^2 - 10p^2 x y + (m^2 - 3p^2)x + (m^2 - 3p^2)y - i\varepsilon} \right. \\
&\quad \left. - \frac{1}{3p^2 x^2 + 3p^2 y^2 - 10p^2 x y - 3p^2 x - 3p^2 y + m^2 - i\varepsilon} \right] \\
&= \frac{1}{16\pi m^2} \int_0^1 dx \int_0^{1-x} dy [\delta(3p^2 x^2 + 3p^2 y^2 - 10p^2 x y + (m^2 - 3p^2)x + (m^2 - 3p^2)y) \\
&\quad - \delta(3p^2 x^2 + 3p^2 y^2 - 10p^2 x y - 3p^2 x - 3p^2 y + m^2)]
\end{aligned}$$

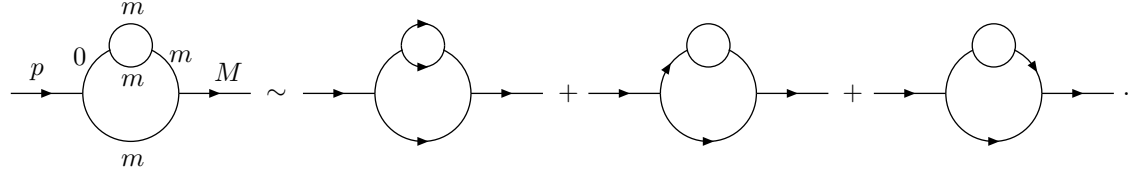
$$\begin{aligned}
&= \frac{\theta[p - \frac{m}{2}]\theta[\frac{m}{\sqrt{3}} - p]}{128\pi m^2 p^2} \ln \frac{9p^3 - m^2 p + 2m^2 \sqrt{4p^2 - m^2}}{9p^3 - m^2 p - 2m^2 \sqrt{4p^2 - m^2}} \\
&+ \frac{\theta[p - \frac{m}{\sqrt{3}}]\theta[\frac{2m}{\sqrt{3}} - p]}{128\pi m^2 p^2} \ln \frac{9p^3 - m^2 p + 2m^2 \sqrt{4p^2 - m^2}}{9(9p^3 - m^2 p - 2m^2 \sqrt{4p^2 - m^2})} \\
&+ \frac{\theta[p - \frac{2m}{\sqrt{3}}]}{128\pi m^2 p^2} \ln \frac{(9p^3 - m^2 p + 2m^2 \sqrt{4p^2 - m^2})(15p^2 + 4p\sqrt{9p^2 - 12m^2} - 4m^2)}{9(9p^3 - m^2 p - 2m^2 \sqrt{4p^2 - m^2})(15p^2 - 4p\sqrt{9p^2 - 12m^2} - 4m^2)}. \tag{10}
\end{aligned}$$

On the other hand, under the ameliorated cutting rules we also have (see Fig.2)

$$\begin{aligned}
&Im(-i) \int \frac{d^4 k}{(2\pi)^4} \frac{1}{k^2 + i\varepsilon} \frac{1}{(k - q)^2 - m^2 + i\varepsilon} \frac{1}{k^2 - m^2 + i\varepsilon} \frac{1}{(k + r)^2 - m^2 + i\varepsilon} \\
&= \frac{1}{8\pi^2} P \int d^4 k \left[\frac{\theta[k_0]\delta(k^2 - m^2)\theta[q_0 + r_0 - k_0]\delta((q + r - k)^2 - m^2)}{(k - r)^2((k - r)^2 - m^2)} + \frac{\theta[k_0]\delta(k^2 - m^2)\theta[r_0 - k_0]\delta((r - k)^2 - m^2)}{k^2((k + q)^2 - m^2)} \right. \\
&\quad + \frac{\theta[k_0]\delta(k^2 - m^2)\theta[q_0 - k_0]\delta((q - k)^2 - m^2)}{k^2((k + r)^2 - m^2)} + \frac{\theta[k_0]\delta(k^2)\theta[r_0 - k_0]\delta((r - k)^2 - m^2)}{(k^2 - m^2)((k + q)^2 - m^2)} \\
&\quad \left. + \frac{\theta[k_0]\delta(k^2)\theta[q_0 - k_0]\delta((q - k)^2 - m^2)}{(k^2 - m^2)((k + r)^2 - m^2)} \right] \\
&= \frac{\theta[p - m/2]}{128\pi m^2 p^2} \ln \frac{9p^3 - m^2 p + 2m^2 \sqrt{4p^2 - m^2}}{9p^3 - m^2 p - 2m^2 \sqrt{4p^2 - m^2}} \\
&+ \frac{\theta[p - 2m/\sqrt{3}]}{128\pi m^2 p^2} \ln \frac{15p^2 - 4m^2 + 4p\sqrt{9p^2 - 12m^2}}{15p^2 - 4m^2 - 4p\sqrt{9p^2 - 12m^2}} - \frac{\theta[p - m/\sqrt{3}]}{64\pi m^2 p^2} \ln 3. \tag{11}
\end{aligned}$$

It is obvious that Eq.(11) is equal to Eq.(10).

Lastly we consider the case of the branch cut simultaneously coming from the dimensional regularization and the singularities of Feynman parameter integrals. A simple Feynman diagram in this case is



Under the conventional integral algorithm and Eq.(4) we have

$$\begin{aligned}
&Im \mu^{2\epsilon} \int \frac{d^D k_1}{(2\pi)^D} \frac{d^D k_2}{(2\pi)^D} \frac{1}{k_1^2 + i\varepsilon} \frac{1}{k_2^2 - m^2 + i\varepsilon} \frac{1}{(k_2 - k_1)^2 - m^2 + i\varepsilon} \frac{1}{k_1^2 - m^2 + i\varepsilon} \frac{1}{(k_1 - p)^2 - m^2 + i\varepsilon} \\
&= \frac{1}{256\pi^4} Im \int_0^1 dx \int_0^1 dy \int_0^{1-y} dz \frac{dz}{M^2 y^2 + (m^2 - M^2)y + m^2 z - i\varepsilon} \left[\Delta + \ln \frac{1-y-z}{x-x^2} \right. \\
&\quad \left. - \ln \left(\frac{M^2 y^2}{m^2} - \frac{M^2 y}{m^2} + y + z + \frac{1-y-z}{x-x^2} - i\varepsilon \right) - \ln \left(\frac{M^2 y^2}{m^2} - \frac{M^2 y}{m^2} + y + z - i\varepsilon \right) \right] \\
&= \frac{1}{256\pi^3} \int_0^1 dx \int_0^1 dy \int_0^{1-y} dz \delta(M^2 y^2 + (m^2 - M^2)y + m^2 z) \left[\Delta + \ln \frac{1-y-z}{x-x^2} \right. \\
&\quad \left. - \ln \left| \frac{M^2 y^2}{m^2} - \frac{M^2 y}{m^2} + y + z + \frac{1-y-z}{x-x^2} \right| \right] \\
&+ \frac{1}{256\pi^3} P \int_0^1 dx \int_0^1 dy \int_0^{1-y} dz \frac{\theta[\frac{M^2 y}{m^2} - \frac{M^2 y^2}{m^2} - y - z - \frac{1-y-z}{x-x^2}]}{M^2 y^2 + (m^2 - M^2)y + m^2 z} \\
&+ \frac{1}{512\pi^3 m^2} Im \int_0^1 dx \int_0^1 dy \left[\ln^2 \left(\frac{M^2 y^2}{m^2} - \frac{M^2 y}{m^2} + y - i\varepsilon \right) - \ln^2 \left(\frac{M^2 y^2}{m^2} - \frac{M^2 y}{m^2} + 1 - i\varepsilon \right) \right] \\
&= \frac{\theta[M - m]\theta[2m - M](M^2 - m^2)}{256\pi^3 m^2 M^2} (\Delta - 2 \ln \frac{M^2 - m^2}{m M} + 2)
\end{aligned}$$

$$\begin{aligned}
& + \frac{\theta[M-2m]\theta[3m-M]}{256\pi^3m^2M^2} \left[(M^2-m^2-M\sqrt{M^2-4m^2})\Delta + 2(M^2-m^2)(1-\ln\frac{M^2-m^2}{mM}) \right. \\
& + M\sqrt{M^2-4m^2}(\ln\frac{M^2-4m^2}{m^2} + \frac{\pi}{\sqrt{3}} - 4) \left. \right] \\
& + \frac{\theta[M-3m]}{256\pi^3m^2M^2} \left[(M^2-m^2-M\sqrt{M^2-4m^2})\Delta + M\sqrt{M^2-4m^2}(\ln\frac{M^2-4m^2}{m^2} + \frac{\pi}{\sqrt{3}} - 4) \right. \\
& \left. + 2(M^2-m^2)(1-\ln\frac{M^2-m^2}{mM}) + 2M^2 \int_{y_1}^{y_2} \left(F - \sqrt{3} \operatorname{tg}^{-1} \frac{F}{\sqrt{3}} \right) dy \right], \tag{12}
\end{aligned}$$

where

$$\begin{aligned}
\Delta &= \frac{2}{\epsilon} + 2\ln 4\pi - 2\gamma - 2\ln \frac{m^2}{\mu^2}, \\
F &= \sqrt{\frac{M^2y^2 - M^2y - 3m^2y + 4m^2}{y(M^2y - M^2 + m^2)}}, \\
y_{1,2} &= \frac{M^2 + 3m^2 \mp \sqrt{M^4 - 10m^2M^2 + 9m^4}}{2M^2}. \tag{13}
\end{aligned}$$

Under the ameliorated cutting rules we also have

$$\begin{aligned}
& Im \mu^{2\epsilon} \int \frac{d^D k_1}{(2\pi)^D} \frac{d^D k_2}{(2\pi)^D} \frac{1}{k_1^2 + i\epsilon} \frac{1}{k_2^2 - m^2 + i\epsilon} \frac{1}{(k_2 - k_1)^2 - m^2 + i\epsilon} \frac{1}{k_1^2 - m^2 + i\epsilon} \frac{1}{(k_1 - p)^2 - m^2 + i\epsilon} \\
& = Im \mu^{2\epsilon} P \int \frac{d^D k_1}{(2\pi)^D} \frac{d^D k_2}{(2\pi)^D} \left[\frac{4i\pi^3 \theta[k_{10}]\delta(k_1^2 - m^2)\theta[k_{20}]\delta(k_2^2 - m^2)\theta[p_0 - k_{10} - k_{20}]\delta((p - k_1 - k_2)^2 - m^2)}{(p - k_1)^2((p - k_1)^2 - m^2)} \right. \\
& \left. - \frac{2\pi^2\theta[k_{10}]\delta(k_1^2)\theta[p_0 - k_{10}]\delta((p - k_1)^2 - m^2)}{(k_1^2 - m^2)((k_2 - k_1)^2 - m^2)(k_1^2 - m^2)} - \frac{2\pi^2\theta[k_{10}]\delta(k_1^2 - m^2)\theta[p_0 - k_{10}]\delta((p - k_1)^2 - m^2)}{k_1^2(k_2^2 - m^2)((k_2 - k_1)^2 - m^2)} \right] \\
& = \frac{1}{64\pi^3} P \int_0^\infty k_1^2 dk_1 \int_0^\infty k_2^2 dk_2 \int_{-1}^1 dx \frac{\delta(M - \sqrt{m^2 + k_1^2} - \sqrt{m^2 + k_2^2} - \sqrt{m^2 + k_1^2 + k_2^2 + 2k_1 k_2 x})}{\sqrt{m^2 + k_1^2} \sqrt{m^2 + k_2^2} \sqrt{m^2 + k_1^2 + k_2^2 + 2k_1 k_2 x}} \\
& \times \frac{1}{(M^2 + m^2 - 2M\sqrt{m^2 + k_1^2})(M^2 - 2M\sqrt{m^2 + k_1^2})} \\
& + \frac{2\pi^2\mu^{2\epsilon}\Gamma(\epsilon/2)}{(4\pi)^{D/2}m^2} \int \frac{d^D k_1}{(2\pi)^D} \theta[k_{10}]\delta(k_1^2)\theta[p_0 - k_{10}]\delta((p - k_1)^2 - m^2) \\
& - \frac{2\pi^2\mu^{2\epsilon}\Gamma(\epsilon/2)}{(4\pi)^{D/2}m^2} \int_0^1 \frac{dx}{(x^2 - x + 1)^{\epsilon/2}} \int \frac{d^D k_1}{(2\pi)^D} \theta[k_{10}]\delta(k_1^2 - m^2)\theta[p_0 - k_{10}]\delta((p - k_1)^2 - m^2) \\
& = \frac{\theta[M-3m]m^2}{64\pi^3 M} \int_1^{\frac{M^3-3m^2}{2mM}} \frac{\sqrt{(x^2-1)(M^2-2mMx-3m^2)}}{(M^2+m^2-2mMx)^{3/2}(M-2mx)} dx \\
& + \frac{\theta[M-m](M^2-m^2)}{256\pi^3m^2M^2} (\Delta - 2\ln\frac{M^2-m^2}{mM} + 2) \\
& - \frac{\theta[M-2m]\sqrt{M^2-4m^2}}{256\pi^3m^2M} (\Delta - \ln\frac{M^2-4m^2}{m^2} + 4 - \frac{\pi}{\sqrt{3}}), \tag{14}
\end{aligned}$$

We note that a similar calculation has been present in Ref.[5]. Numerical results show that Eq.(14) is equal to Eq.(12), as shown in Fig.7.

All of the four examples show that the ameliorated cutting rules agrees with the conventional integral algorithm very well. There are also many such examples which we don't list.

IV. OPTICAL THEOREM AND THE CUTTING RULES

It is well-known that the optical theorem has put a strong constraint on the imaginary part of physical amplitude. Do it agrees with the cutting rules? Usually people think the optical theorem is a straightforward consequent of the

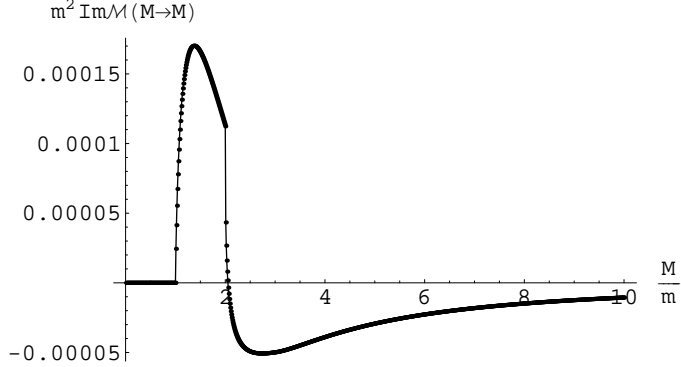


FIG. 7: Results of Eq.(14) (plotted as dot) and Eq.(12) (plotted as line).

unitarity of S-matrix. But things may be not so simple. In the followings we firstly review the derivation of the optical theorem. Inserting $S = 1 + iT$ in the formula $S^\dagger S = 1$ one has:

$$-i(T - T^\dagger) = T^\dagger T. \quad (15)$$

Let us take the matrix element of this equation between two-particle states $|\mathbf{p}_1 \mathbf{p}_2\rangle$ and $|\mathbf{k}_1 \mathbf{k}_2\rangle$ and insert a complete set of intermediate states into the right-hand side:

$$\langle \mathbf{p}_1 \mathbf{p}_2 | T^\dagger T | \mathbf{k}_1 \mathbf{k}_2 \rangle = \sum_f \int d \prod_f \langle \mathbf{p}_1 \mathbf{p}_2 | T^\dagger | f \rangle \langle f | T | \mathbf{k}_1 \mathbf{k}_2 \rangle, \quad (16)$$

where the sum runs over all possible sets f of intermediate states and $d \prod_f$ represents the phase space integrals of f . Then expressing the T-matrix elements as invariant matrix elements \mathcal{M} times 4-momentum-conserving delta functions, one has:

$$\mathcal{M}(k_1 k_2 \rightarrow p_1 p_2) - \mathcal{M}^*(p_1 p_2 \rightarrow k_1 k_2) = i \sum_f \int d \prod_f \mathcal{M}^*(p_1 p_2 \rightarrow f) \mathcal{M}(k_1 k_2 \rightarrow f). \quad (17)$$

Setting $k_i = p_i$ and applying the kinematic factors required by Eq.(17) to build a cross section, one obtains the standard form of the optical theorem:

$$Im \mathcal{M}(k_1 k_2 \rightarrow k_1 k_2) = 2 E_{cm} p_{cm} \sigma_{tot}(k_1 k_2 \rightarrow \text{anything}). \quad (18)$$

If considering the $1 \rightarrow 1$ process we obtain the well-known relationship:

$$Im \mathcal{M}(a \rightarrow a) = m_a \Gamma_a, \quad (19)$$

where m_a and Γ_a are the mass and decay width of particle a . Eq.(19) is in agreement with Eq.(3).

This is the usual derivation of the optical theorem, but there is a serious contradiction. From the unitarity of S-matrix $S^\dagger S = S S^\dagger$ one has

$$T^\dagger T = T T^\dagger. \quad (20)$$

Thus Eq.(16) can be changed to

$$\langle \mathbf{p}_1 \mathbf{p}_2 | T^\dagger T | \mathbf{k}_1 \mathbf{k}_2 \rangle = \sum_f \int d \prod_f \langle \mathbf{p}_1 \mathbf{p}_2 | T | f \rangle \langle f | T^\dagger | \mathbf{k}_1 \mathbf{k}_2 \rangle. \quad (21)$$

Combine Eq.(16) this means for arbitrary intermediate states f

$$\langle \mathbf{p}_1 \mathbf{p}_2 | T^\dagger | f \rangle = \langle \mathbf{p}_1 \mathbf{p}_2 | T | f \rangle, \quad \langle f | T | \mathbf{k}_1 \mathbf{k}_2 \rangle = \langle f | T^\dagger | \mathbf{k}_1 \mathbf{k}_2 \rangle. \quad (22)$$

Since f are arbitrary, we ultimately have

$$\mathcal{M}(k_1 k_2 \rightarrow p_1 p_2) - \mathcal{M}^*(p_1 p_2 \rightarrow k_1 k_2) = 0. \quad (23)$$

Eq.(23) obviously contradicts Eq.(17). Another problem of the optical theorem is: If the charge conjugation is conserved, under the CPT conservation law the l.h.s of Eq.(17) is pure imaginary, but the r.h.s. of Eq.(17) may contain real part which comes from the singularities of the physical amplitudes. Why are there such paradox? In fact as we know, in some specific circumstances radiative corrections can break up some symmetries of the Lagrangian of a quantum field theory [6]. In the present case the radiative corrections just break the symmetry of the optical theorem. In the next section we will see that insisting on the optical theorem will lead to the physical results gauge-parameter dependent.

We can concretely illustrate the paradox of the optical theorem using the physical process $t \rightarrow cZ$. Firstly let us analyze the origination of the imaginary part of physical amplitudes. We know there are two origins to generate the imaginary parts of physical amplitudes: one comes from the imaginary part of the coupling constants, the other comes from the singularities of Feynman propagators which are calculated by the cutting rules. Thus at one-loop level a physical amplitude can be expressed in the form

$$\mathcal{M}(i \rightarrow f) = \sum_k g_k (a_k + i b_k), \quad (24)$$

where the sum runs over different Feynman diagrams, b_k is the imaginary part coming from the contribution of the singularities of Feynman propagators, a_k is a real number not containing the contribution of the singularities of Feynman propagators, and all of the imaginary parts of the coupling constants are included in the coefficient g_k . In the following discussions we call the term $\sum_k g_k b_k$, which represents the contribution of the singularities of Feynman propagators to physical amplitudes, as *quasi-imaginary* part, since it will be pure imaginary if the coefficient g_k , i.e. the products of the coupling constants, are real numbers. Besides, the term $\sum_k g_k a_k$ is called as *quasi-real* part accordingly. Under the charge conjugation transformation only the imaginary parts of the coupling constants change into their contra-values, all of the other quantities in Eq.(24) keep unchanged. Thus use the CPT conservation law we have

$$\mathcal{M}^*(f \rightarrow i) = \mathcal{M}^*(\bar{i} \rightarrow \bar{f}) = \sum_k [g_k^*(a_k + i b_k)]^* = \sum_k g_k (a_k - i b_k). \quad (25)$$

Combine Eq.(24) and Eq.(25) we can easily obtain

$$\tilde{Im}\mathcal{M}(i \rightarrow f) = \sum_k g_k b_k = \frac{1}{2i} (\mathcal{M}(i \rightarrow f) - \mathcal{M}^*(f \rightarrow i)), \quad (26)$$

where \tilde{Im} takes the *quasi-imaginary* part. So under the optical theorem we have

$$\begin{aligned} \tilde{Im}\mathcal{M}(t \rightarrow cZ) &= \frac{1}{2i} (\mathcal{M}(t \rightarrow cZ) - \mathcal{M}^*(cZ \rightarrow t)) \\ &= \frac{1}{2} \sum_f \int d \prod_f \mathcal{M}^*(cZ \rightarrow f) \mathcal{M}(t \rightarrow f). \end{aligned} \quad (27)$$

On the other hand, we can calculate the *quasi-imaginary* part of $\mathcal{M}(t \rightarrow cZ)$ from the Feynman diagrams which are shown in Fig.8. we can readily see that only the first kind cut of Fig.1 is acceptable for the first six diagrams of Fig.8 under the restriction of Eq.(27), because the cuts of the other two kinds of Fig.1 will bring extra contribution $\sim \sum_f \int d \prod_f [\mathcal{M}^*(c \rightarrow f) \mathcal{M}(t \rightarrow Z f) + \mathcal{M}^*(Z \rightarrow f) \mathcal{M}(t \rightarrow c f)]$ to $\tilde{Im}\mathcal{M}(t \rightarrow cZ)$. Eq.(27) also denies the cuts of the $t \rightarrow c$ self-energy diagrams in the seventh and eighth diagrams of Fig.8 for the same reason. But from the derivation of Eq.(19) we find that the cuts of the $t \rightarrow c$ self-energy diagrams in the seventh and eighth diagrams of Fig.8 must be included in $\tilde{Im}\mathcal{M}(t \rightarrow cZ)$. This is an obviously paradox of the optical theorem. One may guess that the optical theorem allows all of the extra cuts, but guarantees the sum of the extra cuts equal to zero. Unfortunately our calculations show that this guess is wrong. After careful calculations of the sum of all of the extra cuts we obtain

$$\begin{aligned} &\bar{c} \ell^* \gamma_L t \sum_i \frac{V_{2i} V_{3i}^* e^3 x_{d,i}}{192\pi c_W s_W^3 (c_W^2 x_t - 1)^2} \left[4x_t^2 c_W^6 + (5x_t^2 - 3x_t - 6)c_W^4 - (6x_t + 7)c_W^2 + 1 \right. \\ &\left. - \frac{c_W^2 \ln(x_t - 1 - 1/c_W^2)}{c_W^2 x_t - 1} (2(x_t - 2)x_t^2 c_W^6 + (x_t^3 - 3x_t^2 + 6)c_W^4 - (2x_t^2 + 7x_t - 10)c_W^2 + x_t + 8) \right] \theta[M_Z - 2m_{d,i}] \\ &+ \bar{c} \frac{\epsilon^* \cdot p_1}{M_W} \gamma_R t \sum_i \frac{V_{2i} V_{3i}^* e^3 x_{d,i} c_W^3 \sqrt{x_t}}{96\pi s_W^3 (c_W^2 x_t - 1)^3} \left[21 + 5x_t + (18 + x_t - 5x_t^2)c_W^2 - 4x_t^2 c_W^4 + \right. \\ &\left. + \frac{\ln(x_t - 1 - 1/c_W^2)}{c_W^2 x_t - 1} (2(x_t - 2)x_t^2 c_W^6 + (x_t^3 - 9x_t^2 - 8x_t + 18)c_W^4 - 2(x_t^2 + x_t - 15)c_W^2 + x_t + 9) \right] \theta[M_Z - 2m_{d,i}] \end{aligned} \quad (28)$$

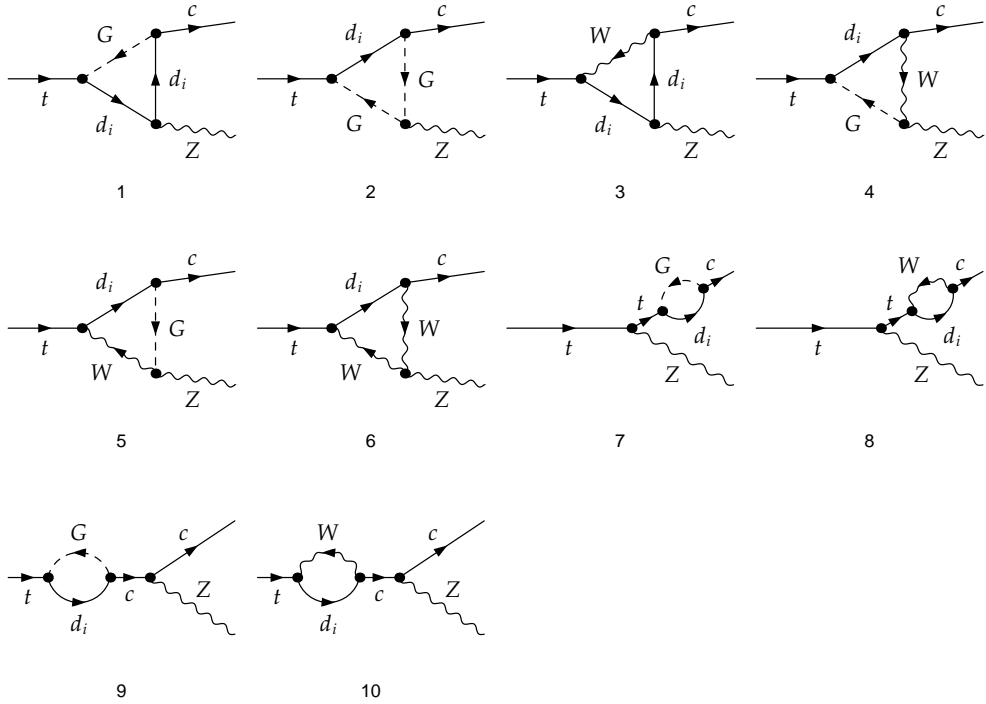


FIG. 8: One-loop diagrams contributing to the physical amplitude of $t \rightarrow cZ$.

where γ_L and γ_R are the left- and right- handed helicity operators, V_{2i} and V_{3i} are CKM matrix elements [7], e is electron charge, s_W and c_W are the sine and cosine of the weak mixing angle, M_Z and M_W are the masses of gauge boson Z and W , $m_{d,i}$ and m_t are the masses of down-type i quark and top quark, and $x_{d,i} = m_{d,i}^2/M_W^2$, $x_t = m_t^2/M_W^2$, and p_1 is the charm quark's momentum. In Eq.(28) we have adopted the approximation $m_c^2/M_W^2 \rightarrow 0$ and expand the result to one order of $x_{d,i}$ since $x_{d,i}$ is very small. Obviously Eq.(28) isn't equal to zero. It represents the contribution of $\sum_f \int d\Gamma_f \mathcal{M}^*(Z \rightarrow f) \mathcal{M}(t \rightarrow c f) / 2$ to $\tilde{I}m \mathcal{M}(t \rightarrow cZ)$.

In fact one readily find that there are many unphysical cuts in Fig.8. The symmetry of gauge theory guarantees the contribution of these unphysical cuts are canceled out each other in the S-matrix elements in a given order [8]. So the optical theorem may make the physical results gauge-parameter dependent, because it discards some possible cuts which may break up the cancellation of the contributions of the unphysical cuts in physical results. In the following section we will discuss this problem.

V. GAUGE DEPENDENCE OF THE PHYSICAL RESULTS UNDER THE OPTICAL THEOREM AND THE AMELIORATED CUTTING RULES

In order to investigate which theorem, the optical theorem or the cutting rules, is acceptable, we calculate two physical amplitudes $t \rightarrow cZ$ and $b \rightarrow s\gamma$ to see which theorem keeps the physical results gauge independent to two-loop level. Since both the two processes have no tree-level contribution, we only need to consider their one-loop Feynman diagrams' contributions.

Firstly we calculate the physical process $t \rightarrow cZ$. We only consider the gauge-dependent part for convenience. Under the ameliorated cutting rules we obtain from Fig.8 (see also Fig.1)

$$\tilde{I}m \mathcal{M}(t \rightarrow cZ)^{ac}|_\xi = 0, \quad (29)$$

where the superscript ac denotes the result is obtained under the ameliorated cutting rules, and subscript ξ takes the gauge-parameter-dependent part of the quantity. Eq.(29) shows that all of the unphysical cuts have been canceled out each other under the ameliorated cutting rules. This coincides with our knowledge. On the other hand, under the optical theorem we obtain

$$\tilde{I}m \mathcal{M}(t \rightarrow cZ)^{op}|_\xi = \bar{c} \not{e}^* \gamma_L t \sum_i \frac{V_{2i} V_{3i}^* e^3 (3 - 4s_W^2) (x_c - \xi_W - x_{d,i})}{384\pi c_W s_W^3 x_c}$$

$$\times \sqrt{x_c^2 - 2(\xi_W + x_{d,i})x_c + (\xi_W - x_{d,i})^2} \theta[m_c - m_{d,i} - M_W \sqrt{\xi_W}], \quad (30)$$

where the superscript *op* denotes the result is obtained under the optical theorem, m_c is the charm quark's mass, and $x_c = m_c^2/M_W^2$. Compared with Eq.(29), the contribution of the second and third cuts of Fig.1 of the first six diagrams of Fig.8 has been discarded in Eq.(30). One can easily see that the r.h.s. of Eq.(30) comes from the unphysical cuts of the seventh and eighth diagrams of Fig.8. These unphysical cuts should be canceled out by the second kind cut of Fig.1 of the first six diagrams of Fig.8, but Eq.(27) eliminates these countervailing terms.

After obtaining the *quasi-real* part of $\mathcal{M}(t \rightarrow cZ)$ by the program packages *LoopTools* [9] we calculate the norm square of $\mathcal{M}(t \rightarrow cZ)$. The numerical results are shown in Fig.9. Here we have used the following input parameters

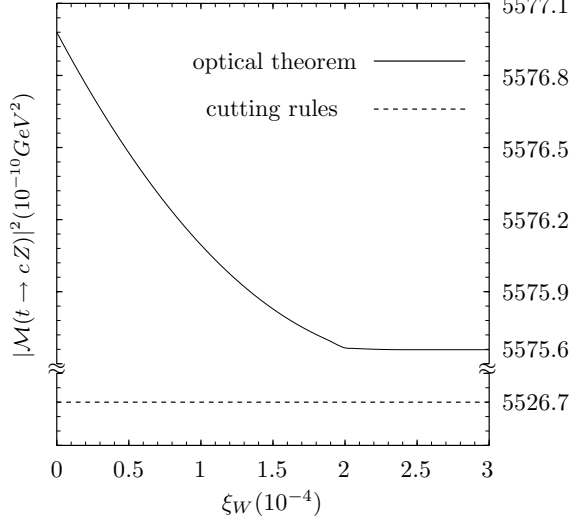


FIG. 9: Gauge dependence of $|\mathcal{M}(t \rightarrow cZ)|^2$ under the optical theorem and the ameliorated cutting rules.

[10]:

- Wolfenstein parameters : $A = 0.819$, $\lambda = 0.2237$, $\rho = 0.230$, $\eta = 0.325$.
- Quark masses: $m_t = 174.3\text{GeV}$, $m_c = 1.25\text{GeV}$, $m_d = 6\text{MeV}$, $m_s = 120\text{MeV}$, $m_b = 4.2\text{GeV}$.
- Other physical constants: $\alpha(M_W^2) = 1/128$, $s_W^2 = 0.23147$, $M_W = 80.419\text{GeV}$, $M_Z = M_W/c_W$.

From Fig.9 one can easily see that the optical theorem leads the decay width of $t \rightarrow cZ$ gauge-parameter dependent, whereas the ameliorated cutting rules keeps it gauge-parameter independent.

Secondly we calculate the physical process $b \rightarrow s\gamma$. From Fig.10 we find that there are only unphysical cuts contributing to the one-loop amplitude of $b \rightarrow s\gamma$. These unphysical cuts should be canceled out each other in the final physical results [8]. Since there is no tree-level contribution, this means these unphysical cuts should be canceled out in the one-loop amplitude of $b \rightarrow s\gamma$. After careful calculations we obtain under the ameliorated cutting rules

$$\tilde{Im}\mathcal{M}(b \rightarrow s\gamma)^{ac} = 0. \quad (31)$$

This coincides with our conclusion. But under the optical theorem we obtain

$$\begin{aligned} \tilde{Im}\mathcal{M}(b \rightarrow s\gamma)^{op} &= \bar{s}\not{e}^*\gamma_L b \sum_i \frac{V_{i3}V_{i2}^* e^3 (x_s - \xi_W - x_{u,i})}{192\pi s_W^2 x_s} \\ &\times \sqrt{x_s^2 - 2(\xi_W + x_{u,i})x_s + (\xi_W - x_{u,i})^2} \theta[m_s - m_{u,i} - M_W \sqrt{\xi_W}], \end{aligned} \quad (32)$$

where m_s and $m_{u,i}$ are the masses of strange quark and up-type i quark, and $x_s = m_s^2/M_W^2$, $x_{u,i} = m_{u,i}^2/M_W^2$. Compared with Eq.(31), the contribution of the second and third cuts of Fig.1 of the first six diagrams of Fig.10 has been discarded in Eq.(32). Obviously the r.h.s of Eq.(32) comes from the unphysical cuts of the seventh and eighth diagrams of Fig.10. They should be canceled out by the unphysical cuts of the second kind cut of Fig.1 of the first six diagrams of Fig.10, but the optical theorem eliminates these countervailing terms.

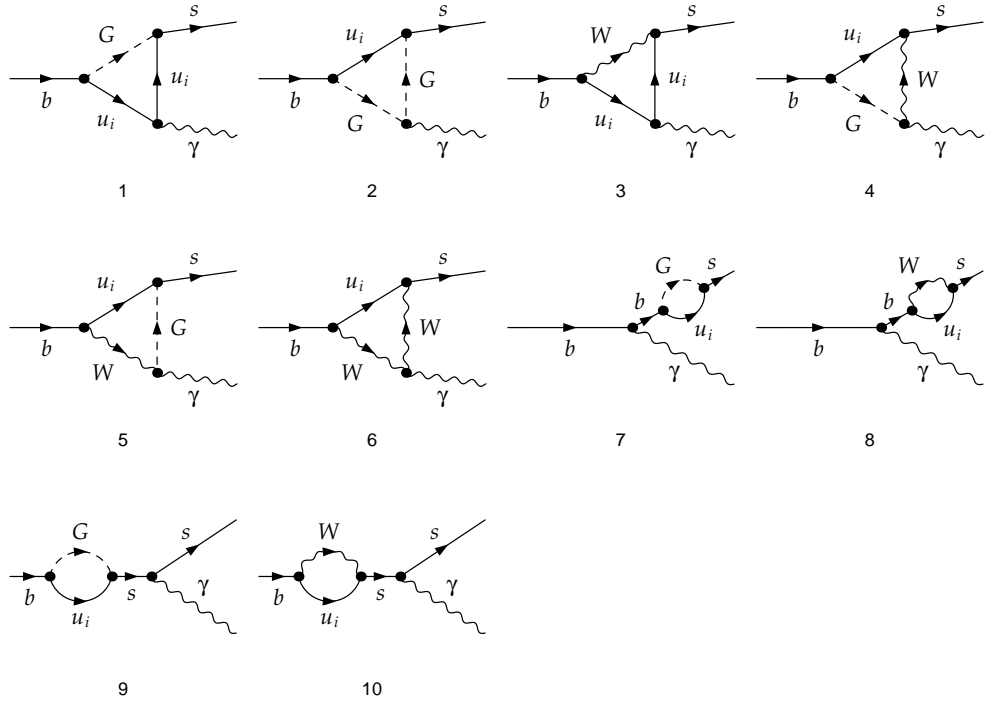


FIG. 10: One-loop diagrams contributing to the physical amplitude of $b \rightarrow s \gamma$.

Since there is no *quasi*-imaginary part in the one-loop amplitude of $b \rightarrow s \gamma$, the gauge invariance of the decay width of $b \rightarrow s \gamma$ requires the *quasi*-real part of the one-loop amplitude of $b \rightarrow s \gamma$ must be gauge-parameter independent. From Eq.(32) this means the optical theorem leads to the decay width of $b \rightarrow s \gamma$ gauge-parameter dependent to two-loop level.

VI. CONCLUSION

In order to calculate the contributions of the singularities of Feynman propagators to Feynman amplitude we investigate the cutting rules, the conventional integral algorithm and the optical theorem. We ameliorate the cutting rules to make it suitable for actual calculations and give accurate result of the imaginary part of unstable particle's self-energy amplitude. The calculations of several Feynman diagrams' imaginary parts show that the ameliorated cutting rules agrees with the conventional integral algorithm very well (see Fig.6,7 and Eq.(8,9,10,11)). On the other hand, through careful investigation we find that the optical theorem is broken by the singularities of physical amplitude. The concrete calculations of the physical processes $t \rightarrow c Z$ and $b \rightarrow s \gamma$ show that the ameliorated cutting rules keeps the decay widths of the physical processes gauge-parameter independent, but the optical theorem leads them gauge-parameter dependent (see Fig.9 and Eqs.(31,32)).

We note that although Feynman diagrams don't represent real physical processes, they still provide a physical picture to describe the virtual processes occurring in the quantum field vacuum. The ameliorated cutting rules fixes the contributions of the *on-shell* virtual processes in the quantum field vacuum to physical amplitudes, thus it will be helpful to discover the deep-seated physical meanings of the quantum field theory.

Acknowledgments

The author thanks Prof. Cai-dian Lu for the fruitful discussions and the corrections of the words. The author also

thanks Yue-long Shen, doctor Jian-feng Cheng, Xian-qiao Yu, Ge-liang Song and Ying Li for the fruitful discussions.

[1] H. Epstein and V. Glaser, Ann. Inst. Poincare **A** **29** (1973) 211;
 R.F. Streater and A.S. Wightman, “PCT, Spin and Statistics, and All That,” Benjamin, New York/Amsterdam, 1964;
 F. Constantinescu, “Distributionen und ihre Anwendung in der Physik,” Teubner, Stuttgart, 1974.

[2] R.E. Cutkosky, J. Math. Phys. **1**, 429 (1960).

[3] G.'t Hooft and M.J.G. Veltman, Nucl. Phys. **B44**, 189 (1972).

[4] D. Wackerlo, W. Hollik, Phys. Rev. **D55** (1997) 6788;
 R.J. Eden, P.V. Landshoff, D.I. Olive, J.C. Polkinghorne, *The Analytic S-Matrix*, Cambridge University Press 1966.

[5] Andreas Aste, Annals of Physics **257** (1997) 158;
 G. Scharf, “Finite Quantum Electrodynamics, the Causal Approach,” 2nd ed., Springer, Berlin/Heidelberg/New York, 1995.

[6] S. Adler and W.A. Bardeen, Phys. Rev. **182** (1969) 1517; S. Adler, in Deser, et. al. (1970).

[7] N. Cabibbo, Phys. Rev. Lett. **10**, 531 (1963);
 M. Kobayashi and K. Maskawa, Prog. Theor. Phys. **49** (1973) 652.

[8] C. Becchi, A. Rouet, and R. Stora, Ann. Phys. **98** (1976) 287;
 I.V. Tyutin, Lebedev Institute preprint (1975, unpublished);
 M.Z. Iofa and I.V. Tyutin, Theor. Math. Phys. **27** (1976) 316;
 T. Kugo and I. Ojima, Prog. Theor. Phys. **66** (1979) 1.

[9] J. Kublbeck, M. Bohm, A. Denner, Comput. Phys. Commun. **60** (1990) 165;
 G.J. van Oldenborgh, J.A.M. Vermaelen, Z. Phys. **C46** (1990) 425;
 T. Hahn, M. Perez-Victoria, Comput. Phys. Commun. **118** (1999) 153.

[10] M. Ciuchini, et. al., JHEP 0107 (2001) 13.